Journal of Solid State Chemistry 182 (2009) 3299–3304

Contents lists available at ScienceDirect

Journal of Solid State Chemistry

journal homepage: www.elsevier.com/locate/jssc

Electronic structure and photoluminescence properties of Eu^{2+}-activated Ca_2BN_2F

Y.Q. Li [a,b,*], C.M. Fang [c], Y. Fang [b], A.C.A. Delsing [a,d], G. de With [a], H.T. Hintzen [a,d]

[a] Laboratory of Materials and Interface Chemistry, Eindhoven University of Technology, P.O. Box 513, 5600 MB, Eindhoven, The Netherlands
[b] College of Materials Science and Engineering, Nanjing University of Technology, Nanjing 210009, China
[c] Kavli Institute of Nanoscience, Delft University of Technology, Lorentzweg 1, 2628 CJ, Delft, The Netherlands
[d] Materials and Devices for Sustainable Energy Technologies, Department of Chemical Engineering and Chemistry, Eindhoven University of Technology, P.O. Box 513, 5600 MB, Eindhoven, The Netherlands

ARTICLE INFO

Article history:
Received 14 June 2009
Received in revised form
7 September 2009
Accepted 20 September 2009
Available online 30 September 2009

Keywords:
Calcium boron–nitride–fluoride
First principles
Electronic structure
Europium
Luminescence

ABSTRACT

The electronic structure of undoped and luminescence properties of Eu^{2+}-doped Ca_2BN_2F have been investigated. First-principles calculations for Ca_2BN_2F show that the valence band is mainly composed of F and N 2*p*, B 2*s* and 2*p* orbitals, while the Ca 4*s* and 3*d* are almost empty, indicating that Ca_2BN_2F is a very ionic compound. The valence band close to the Fermi level is dominated by the N 2*p* states, and the bottom of the conduction band is determined by the Ca 3*d* and N/B 3*s* orbitals. The direct energy gap is calculated to be about 3.1 eV, in fair agreement with the experimental data of ~3.6 eV derived from the diffuse reflection spectrum. Due to the high degree of ionic bonding of the coordinations of Eu with (N, F) on the Ca sites, Ca_2BN_2F:Eu^{2+} shows strong blue emission with a maximum at about 420 nm upon UV excitation in the absorption range of 330–400 nm.

1. Introduction

Alkaline earth nitride compounds can be roughly classified into three catalogs: metal nitride, ionic nitride and covalent nitride, according to the bonding characteristics [1–6]. The luminescence properties of Eu^{2+} in the binary alkaline earth metal nitrides (e.g., Ca_3N_2, SrN_2, BaN_2) hardly can be observed due to a small band gap and significantly higher absorption of the host lattice. Whereas in the covalent nitrides the alkaline earth ions are normally located within the three-dimensional structure of Si–N and Al–N. Eu^{2+}-doped alkaline-earth silicon nitride/oxynitride materials are the typical examples, which are well-known wavelength conversion phosphors for applications in white LED lighting [7–18]. Among such kinds of hosts, there are more opportunities to find novel phosphors emitting in green to red spectral range having unusual long-wavelength excitation bands (370–480 nm). This is attributed to the presence of nitrogen due to high degree of covalent bonding and large crystal field splitting of the 5*d* levels of the Eu^{2+} ion as well as the rigid lattices [19]. Apart from the silicon nitride-based compounds, it is interesting to know the luminescence properties of rare-earth doped nitrogen containing compounds having relatively "soft" elements, like Al and B. It is also interesting to understand the effect of the nitrogen atoms mixed with other types of anions besides oxygen (e.g., beyond the oxynitride compounds), such as F and Cl, on the luminescence properties when these atoms are involved into the first nearest neighbors of the alkaline earth ions. In between ionic and covalent nitrides, Ca_2BN_2F just provides a nice example for our present study combined with its good chemical stability in air.

Ca_2BN_2F crystallizes in the orthorhombic system with space group of *Pnma* and its structure is built by isolated linear nitridoborate anions BN_2^{3-} and $[CaCa_{3/3}F]$ units [20]. There are two different Ca crystallographic sites having sixfold coordination with the nitrogen and fluoride ions in different N/F ratio (N/F=5/1 and 3/3 for Ca1 and Ca2, respectively). The shortest bond lengths are 2.341 and 2.339 Å, respectively, for Ca–N and Ca–F. Additionally, the B–N distances in the (BN_2^{3-}) cluster are significant shorter (i.e., 1.316–1.35 Å). It is well known that the degree of covalent bonding between the alkaline earth ion and ligand is significantly decreased going from N via O to F due to an increase in the electronegativity in a sequence of N (3.04) < O (3.44) < F (3.98) [21]. Therefore, in contrast to rigid lattices of alkaline-earth silicon nitride compounds (e.g., $MSiN_2$ [22], $M_2Si_5N_8$ [5] and $MAlSiN_3$ [14–16] (*M*=Ca, Sr, Ba)) and alkaline-earth silicon oxynitride compounds (e.g., $MSi_2O_2N_2$ (*M*=Ca, Sr, Ba) [9,17,23]), Ca_2BN_2F is a more ionic compound due to the presence of (BN_2^{3-}) and F^- anions

* Corresponding author at: Laboratory of Materials and Interface Chemistry, Eindhoven University of Technology, P.O. Box 513, 5600 MB, Eindhoven, The Netherlands.
E-mail address: li.yuanqiang@nims.go.jp (Y.Q. Li).

0022-4596/$ - see front matter © 2009 Elsevier Inc. All rights reserved.
doi:10.1016/j.jssc.2009.09.028

around Ca [20]. In addition, similar to alkaline earth silicon oxynitride, the addition of F would result in the emission band of Eu^{2+} shifting to shorter wavelength if Eu^{2+} experiences similar environment as expected. It has been found that with Eu^{2+} in pure fluorine environment CaF_2:Eu^{2+} shows blue emission at about 425 nm upon UV excitation [24]. Under N/B environment, BN:Eu^{2+} shows yellow emission with the maximum emission band at 550–560 nm when excited by 365 nm light [25]. Nanotube BN:Eu^{2+}, however, has been found to give blue–green cathode-luminescence at about 490 nm [26]. In contrast with the covalent nitride compounds, so far less attention has been paid to the ionic nitride compounds as the potential luminescent hosts. Our interesting point is concentrated on the luminescence properties of Eu^{2+} that is incorporated into the complex environment aside from only nitrogen atoms, e.g., a combination of CaF_2 and BN. As far as we know, no relevant paper about the luminescence properties of Eu^{2+}-doped Ca_2BN_2F has been published so far. Therefore, in the present study, we firstly performed first-principles calculations to investigate the electronic structures of Ca_2BN_2F for a better understanding of chemical bonding and the luminescence properties. Then we synthesized $Ca_{2-x}Eu_xBN_2F$ compounds by a solid-state reaction under a N_2/H_2 atmosphere. Subsequently, the structural characteristics, optical and photoluminescence properties of $Ca_{2-x}Eu_xBN_2F$ were studied in detail.

2. Experimental procedures

2.1. Synthesis

Undoped and Eu^{2+}-doped Ca_2BN_2F powders were prepared by a solid state reaction. Ca_3N_2 (Alfa, purity $>98\%$), BN (Cedimx, 99%), CaF_2 (Aldrich, $>99.5\%$) and EuN were used as starting materials. The binary nitride EuN was pre-synthesized by nitridation of Eu metal (Csre, $\sim$99%) at 850 °C for 10 h in a horizontal tube furnace under flowing dried nitrogen. Subsequently, the stoichiometric amounts of Ca_3N_2, BN and CaF_2 as well as EuN were weighed out, and then thoroughly mixed and ground in an agate mortar in a dry glovebox flushed with high purity nitrogen because of air and moisture sensitivity of Ca_3N_2 and EuN. For Eu^{2+}-doped Ca_2BN_2F, the Eu concentrations were set at 0.5–1.5 mol% with respect to the Ca^{2+} ion in Ca_2BN_2F. The powder mixtures were then fired in a molybdenum crucible at 1050–1100 °C for 6–8 h in a horizontal tube furnace under a N_2–H_2 (10%) atmosphere. After heating, the samples were gradually cooled down in the furnace.

2.2. Characterizations

The obtained samples were checked by X-ray powder diffraction (Rigaku, D/MAX-B) using Cu$K\alpha$ radiation at 40 kV and 30 mA with a graphite monochromator in the range of 10° and 80° 2θ by a step scan mode (a step size of 0.02° in 2θ and a count time of 2 s). The structural parameters were determined by the Rietveld method using GSAS package [27].

The diffuse reflectance, emission and excitation spectra of the samples were measured at room temperature by a Perkin Elmer LS 50B spectrophotometer equipped with a Xe flash lamp. The reflection spectra were calibrated with the reflection of black felt (reflection 3%) and white barium sulfate ($BaSO_4$, reflection $\sim$100%) in the wavelength region of 230–700 nm. The emission spectra were corrected by dividing the measured emission intensity by the ratio of the observed spectrum of a calibrated W-lamp and its known spectrum from 300 to 900 nm. Excitation spectra were automatically corrected for the variation in the lamp intensity by a second photomultiplier and a beam-splitter. All the spectra were recorded with a scan speed of 200 nm/min at room temperature.

2.3. Density functional theory (DFT) calculations

First-principles calculations [28,29] were carried out in the generalized gradient approximation (GGA) [30] and the local density approximation (LDA) [31] using the projector-augmented wave (PAW) method [31,32], which were preformed by the *ab initio* quantum-mechanical molecular dynamics simulation code of VASP package based on the DFT computations [32]. The electronic wave functions were sampled on a $(4\times10\times4)$ mesh in the irreducible Brillouin zone (BZ) [33]. The cut-off energy of the wave functions was 850 eV. The augment cut-off energy was 900 eV. Convergence of the total energy with the number of the k-mesh and the plane wave cut-off energy has been checked.

3. Results and discussion

3.1. Electronic structure calculations

The optimized lattice parameters of Ca_2BN_2F within both GGA and LDA are listed in Table 1. Compared with our experimental data for powders and literature data for single crystal [20], the GGA values are slightly larger while the LDA values are slightly smaller. As the GGA values are much closer to the experimental data, thus we used the GGA for next studies.

Fig. 1 shows the partial and total density of states (DOS) for Ca_2BN_2F from the GGA. The calculated distribution curves along the high symmetry lines are shown in Fig. 2. The semicore level 2*s* orbitals of the F and N atoms form narrow bands (of band-widths of typically 0.5 eV), which are about 23.5 eV (F 2*s*), or about 13.0 eV (N atoms) below the Fermi level which is set to be the top of the valence band. Also the semicore level Ca 3*p* electrons are calculated to be about 20 eV below the Fermi level. The valence bands are mainly composed of F/N 2*p*, B 2*s* and 2*p* orbitals, as shown in Figs. 1 and 2. The F 2*p* orbitals form a rather narrow band with three peaks at about -5.2, -4.8, and -4.5 eV with the same intensity. The N 2*s* orbitals, which are strongly hybridized with the N 2*p* electron, form a band in the energy range between -4.3 and -3.7 eV. These properties are very similar to two similar ionic compounds of Mg_2NF and Mg_3NF_3 regarding to the energy levels of the F 2*p* and N 2*s*, while the N 2*p* states in Mg_2NF and Mg_3NF_3 are narrowly distributed in the -2.5 to 0 eV range [34]. The relatively high intensity of the Ca2 3*d* orbitals are overlapping with the F 2*p* orbitals within the range of -5.5 to -4.2 eV (Fig. 1), giving an evidence that the chemical bonding between the Ca2 and F atoms is relatively stronger than that

Table 1
Lattice parameters for $Ca_{2-x}Eu_xBN_2F$ (x=0 and 0.02).

$Ca_{2-x}Eu_xBN_2F$	Lattice parameters			
	a (Å)	b (Å)	c (Å)	V (Å^3)
Calc. (x=0)[a]				
GGA	9.2281	3.6718	10.0136	339.3
LDA	8.9526	3.5574	9.7571	310.74
Exp. (x=0, powder)	9.1812(7)	3.6575(2)	9.9657(7)	334.66(4)
Exp. (x=0, single crystal)[b]	9.182(2)	3.649(2)	9.966(2)	333.9(1)
Exp. (x=0.02, powder)	9.1870(4)	3.6603(2)	9.9667(5)	335.15(3)

[a] First-principles calculation data based on PAW-GGA and PAW-LDA.
[b] Single crystal data from Ref. [20].

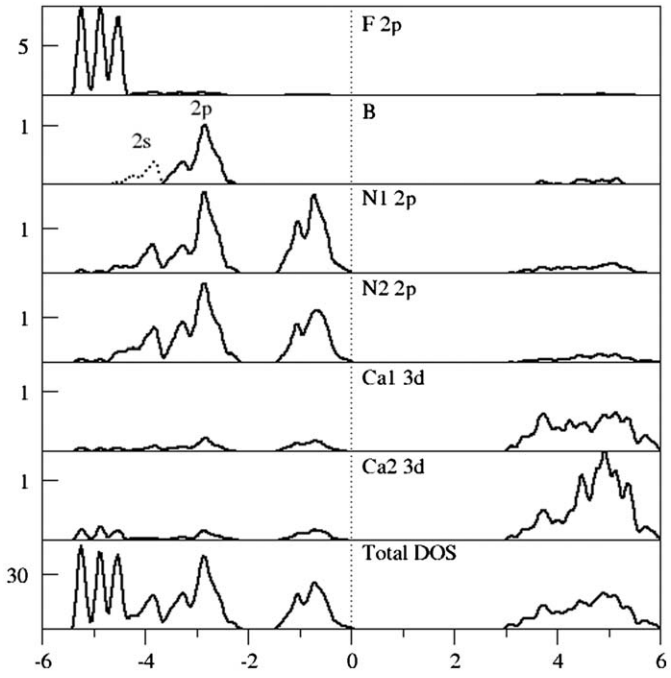

Fig. 1. Partial and total DOS for the valence bands of Ca_2BN_2F.

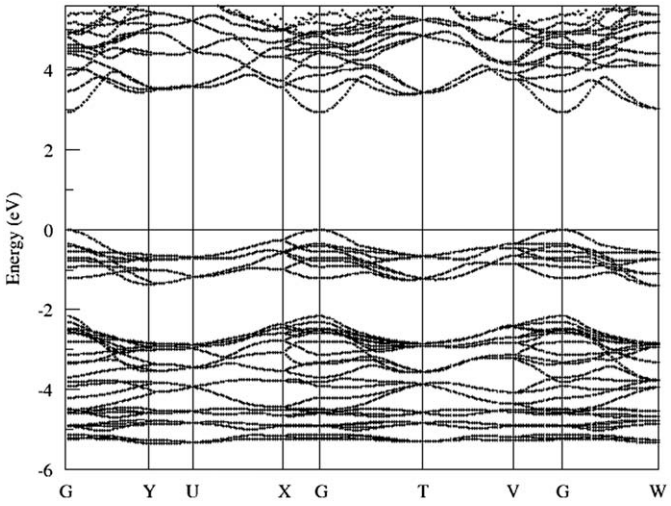

Fig. 2. Dispersion curves close to the Fermi level along the high symmetry lines.

between the Ca1 and F atoms. The B 2*p* orbitals are also strongly hybridized with N 2*p* states, and form a band between about −3.5 and −2.2 eV. That indicates that the B and N atoms are strongly chemically bonded and can be regarded as $(BN_2)^{3-}$ clusters. Beyond hybridizing with the B 2*s* and 2*p*, the remaining N 2*p* orbitals occupied by electrons form a band at the top of the valence band from about −1.4 eV to the Fermi level. The calculated electronic configurations also showed that the Ca 4*s* and 3*d* orbitals are almost empty (forming the conduction band). Therefore, Ca_2BN_2F is a ionic compound which can be formulated to be $Ca^{2+}(BN_2)^{3-}F^-$.

As shown in Figs. 1 and 2, there is a direct energy gap at Γ in the BZ between the top of the valence band and the conduction band. The energy gap is calculated to be about 3.1 eV. The upper part of the valence band is mainly composed of N 2*p* states, while the bottom of the conduction band consists of mainly Ca 3*d* characters. However, the former calculations for the ionic compounds such as Mg_3N_2 showed that the bottom of the conduction band is mainly determined by the unoccupied N 3*s* states [35]. It is reasonable to assert that for $Ca^{2+}(BN_2)^{3-}F^-$ the bottom of the conduction band is composed of Ca 3*d* and very weak N/F 3*s* states. This is largely different with that of Mg_2NF and Mg_3NF_3, where the bottom of the conduction band is determined mainly by the 3*s* states of F and N in the magnesium nitride–fluorides, and the Mg 2*p* states are deep in energy below the Fermi level (~40 eV) [34].

3.2. Phase formation and structural characters

Fig. 3 shows the typical X-ray powder diffraction (XRD) pattern of $Ca_2BN_2F:Eu^{2+}$ (1 mol%). It can be clearly seen that the prepared $Ca_{2-x}Eu_xBN_2F$ is a nearly single phase compound, well matching with the calculated XRD data or a JCPDS 89-4591 card. As a result, the lattice parameters of the powder samples of undoped Ca_2BN_2F are in good agreement with the single crystal data and close to the results calculated by first-principles approaches (Table 1). Moreover, as expected, the lattice parameters of Eu^{2+}-doped Ca_2BN_2F are slightly increased compared with undoped Ca_2BN_2F due to the replacement of small Ca^{2+} ion (1.01 Å, C.N.=7) by the larger Eu^{2+} ion (1.28 Å, C.N.=7) [36], indicating that the Eu^{2+} ion have been incorporated into the Ca_2BN_2F lattice and formed a solid solution. Based on the fact that Sr_2BN_2F is isostructural with Ca_2BN_2F [20], the Eu^{2+} ions should occupy on the two individual Ca sites as shown in Fig. 4 due to similar ionic size of Eu^{2+} and Sr^{2+}. Accordingly, in the structure of $Ca_2BN_2F:Eu^{2+}$ (1 mol%) based on the Rietveld refinement of the powder XRD data, the Eu^1_{Ca} ion is directly coordinated with one F and five N atoms with the average bond length of about 2.505 Å; while the Eu^2_{Ca} ion is coordinated with three F and three N atoms with a shorter average bond length of about 2.416 Å. Both the two Eu_{Ca} sites have the point group of C_1 and the calculated coordination-polyhedron volume [37] for $Eu^1_{Ca}N5F1$ and $Eu^2_{Ca}N3F3$ are about 20.59 and 17.62 $Å^3$, respectively, which has more significant difference in volume upon the two crystallographic sizes. Consequently, the Eu–(N, F) bond has more ionic character in comparison with the Eu–N bond because the electronegativity of F (3.98) is higher than that of N (3.04). Specifically, Eu^2_{Ca}–(N, F) has higher degree of ionic bonding than that of Eu^1_{Ca}–(N, F) due to the presence of more coordinating F atoms with shorter $Eu^2_{Ca}-F$ bond distances (Fig. 4) in $Ca_{2-x}Eu_xBN_2F$. Therefore, it would be expected that these local structure characters would have greatly influences on the luminescence properties of Eu^{2+}.

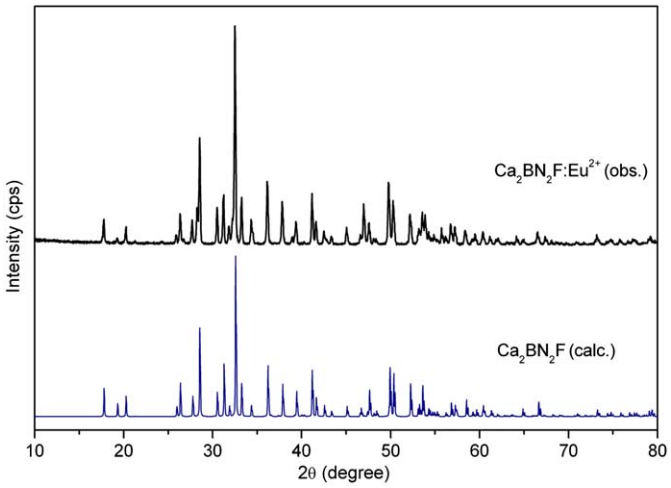

Fig. 3. Observed and calculated X-ray powder diffraction patterns of $Ca_2BN_2F:Eu^{2+}$ (1 mol%) and Ca_2BN_2F.

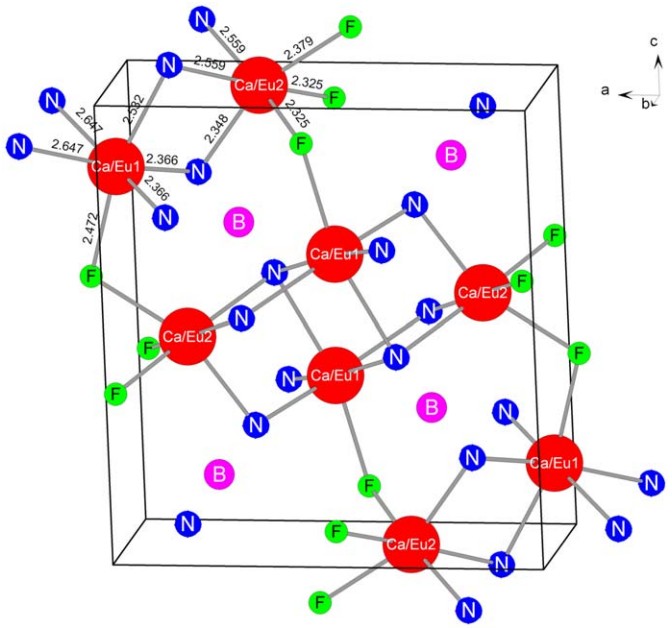

Fig. 4. Projection of the crystal structure of $Ca_2BN_2F:Eu^{2+}$ and Eu_{Ca}-(N, F) bond length (Å).

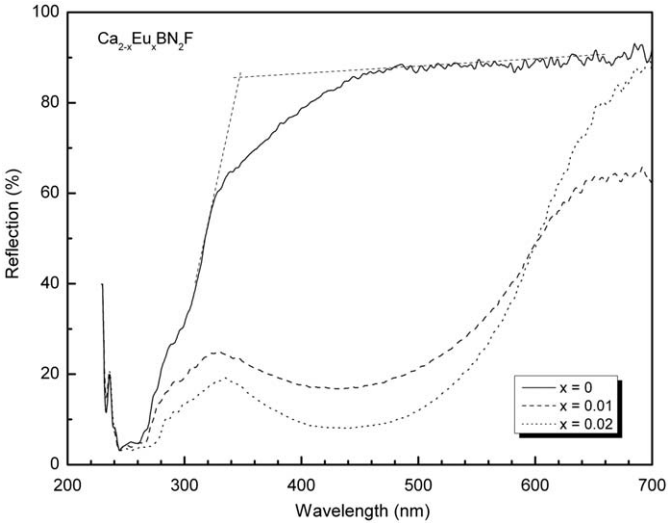

Fig. 5. Diffuse reflection spectra of undoped and Eu^{2+}-doped Ca_2BN_2F.

3.3. *Luminescence properties of $Ca_2BN_2F:Eu^{2+}$*

Fig. 5 illustrates the diffuse reflection spectra of undoped and Eu^{2+}-doped Ca_2BN_2F. The reflection intensity of undoped Ca_2BN_2F is as high as ~90% in the spectral range of 450–700 nm, and then shows a gradual decrease within 450–310 nm, implying a weak absorption of the host in the visible range. A sharp drop can be clearly observed approximately from 310 to 260 nm in the UV partition of the reflection spectrum of Ca_2BN_2F originating from the electron transition from the valence to the conduction band. This is in agreement with the observation of a grayish-white daylight color for undoped Ca_2BN_2F powder. The optical band gap of Ca_2BN_2F was estimated to be about 3.6 eV from the diffuse reflection spectrum (the intersection point of two extrapolation lines of the reflection spectrum in the ranges of 480–700 and 250–320 nm, as shown in Fig. 5), roughly in correspondence with the value (~3.1 eV) obtained by first-principles calculations (see Section 3.1). Based on the fact that the limitation of the DFT

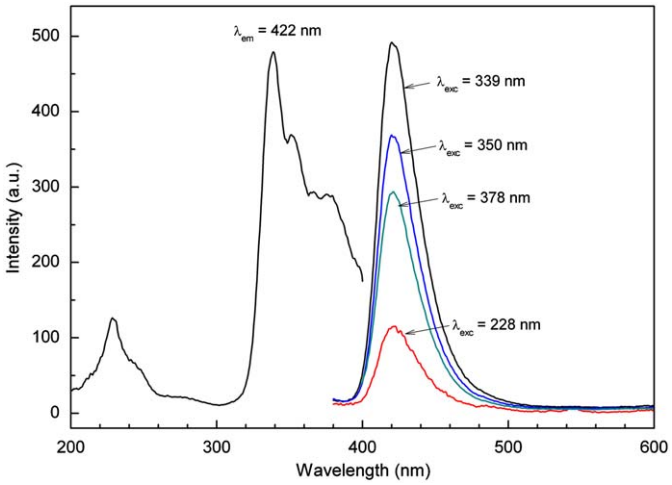

Fig. 6. Excitation and emission spectra of $Ca_2BN_2F:Eu^{2+}$ (0.5 mol%).

calculations in the description of the excitation states in solids, this underestimated band gap is understood for the first-principles calculations.

Eu^{2+}-doped Ca_2BN_2F has a strong absorption band superimposed on the reflection spectrum of undoped Ca_2BN_2F, broadly covering the visible range from 330 to 660 nm. This broad absorption band is readily assigned to the Eu^{2+} ion because both the host and the Eu^{3+} ion do not have absorption in this range. Accordingly, the observed daylight color of $Ca_2BN_2F:Eu^{2+}$ powder is orangish-yellow pigment with the CIE color points at (0.41, 0.38) and (0.48, 0.39) for $Ca_2BN_2F:Eu^{2+}$ (0.5 mol%) and $Ca_2BN_2F:Eu^{2+}$ (1 mol%), respectively.

Even though there is a strong Eu^{2+} absorption band in the visible range of 360–650 nm centered at about 450 nm (Fig. 5), the absorbed energy does not lead to excitation (Fig. 6) probably because this Eu^{2+} center has been quenched at room temperature. As a result, this Eu^{2+} center cannot convert efficiently the absorbed energy into electromagnetic radiation of a different wavelength. The excitation spectrum consists of two major excitation bands located in the UV (200–280 nm) peaking at about 229 and 245 nm, and the visible light range (320–450 nm) peaking at 339, 351, 367, 378 nm having a large separation with the UV ones in wavelength. According to the reflection spectra (Fig. 5), the first excitation band at 229 nm could be assigned to the host excitation band as this band is deeply inside the absorption edge of Ca_2BN_2F. Other excitation bands in the visible range are ascribed to the Eu^{2+} ions. On the other hand, the excitation band clearly shows efficient excitation at about 339 nm, indicating a second Eu^{2+} center, in agreement with the presence of two Ca crystallographic sites in the host lattice [20]. Because this Eu center (~339 nm) does not show up outstandingly in the reflection spectrum, this suggests that the concentration of this Eu center maybe very low. On the basis of those facts, the long wavelength absorption at around 450 nm (not observable in the excitation spectrum) is probably ascribed to the covalent $Eu^1_{Ca}N5F1$ center, while the short wavelength excitation band at about 339 nm could be ascribed to the ionic $Eu^2_{Ca}N3F3$ center.

Nitrogen seems to be having large impact on the Eu^{2+} ions, since the intensity of the dominant excitation bands of Eu^{2+} in the range of 320–420 nm is much higher than that at around 230 nm for $Ca_2BN_2F:Eu^{2+}$ even in the presence of the higher electronegative F atoms. From the excitation spectra, the estimated crystal field splitting (CFS, the energy difference between highest and lowest observed 5*d* excitation bands of Eu^{2+} in energy) is

Table 2
Luminescence characters of Eu^{2+} doped Ca_2BN_2F, calcium silicon nitrides and oxynitride as well as CaF_2.

Materials	Excitation λ_{exc}^{max} (nm)	Emission λ_{em}^{max} (nm)	CFS (cm^{-1})	COG (cm^{-1})	Stokes shift (cm^{-1})
Ca_2BN_2F	339	422	14 360	31 000	2800
$CaSiN_2$ [38]	360	630–655	14 000	25 100	5000
$Ca_2Si_5N_8$ [11]	394	605–620	13 500	25 800	5100
$CaSi_2N_2O_2$ [17]	395	560	15 700	29 000	4500
CaF_2 [24]	~350	425	N/A	N/A	~5040

about 14 360 cm^{-1}, and the center of gravity (COG, average energy of the observed 5*d* excitation levels of Eu^{2+}) is about 31 000 cm^{-1}. In comparison with $CaSiN_2$:Eu^{2+} [38], their CFS values are comparable, while the COG value of Ca_2BN_2F:Eu^{2+} is much higher than that of $CaSiN_2$:Eu^{2+} (~25 100 cm^{-1}), reflecting more ionic bonds of Eu_{Ca}-(N, F) in Ca_2BN_2F:Eu^{2+} as described above. Similarly, as compared with other calcium–silicon–nitride/oxynitride phosphors, Ca_2BN_2F:Eu^{2+} also has the highest COG values having similar CFS values, as listed in Table 2. Ca_2BN_2F:Eu^{2+} shows strong deep blue emission peaking at about 422 nm which is ascribed to the transition of $4f^6 5d \rightarrow 4f^7$ ($8S_{7/2}$) of Eu^{2+} [39]. In addition, the position of the emission band of Eu^{2+} is nearly independent of the excitation wavelengths (see Fig. 6) in agreement with an assumption that only the Eu_{Ca}^2N3F3 center does show luminescence. Just from the positions of the emission and excitation bands of Eu^{2+}, it seems that the luminescence characteristics of Ca_2BN_2F:Eu^{2+} are much similar to that of CaF_2:Eu^{2+}, which further implies that the overall Eu^{2+} luminescence properties of the Eu_{Ca}^2N3F3 center in Ca_2BN_2F:Eu^{2+} are dominated by the F^- ions due to its significantly shorter distances (e.g., Eu_{Ca}–F for Eu^{2+} 1 mol%: 2.325, 2.325, and 2.379 Å) than that of the N^{3-} ions. It is worth noting that generally the emission bands of Eu^{2+} are located at nearby or above the absorption edge of Eu^{2+} (in wavelength), as found in $M_2Si_5N_8$:Eu^{2+} and $CaSiN_2$:Eu^{2+}, etc. [11,38]. However, for Ca_2BN_2F:Eu^{2+} both the dominant excitation band (~339 nm) and the emission band (~422 nm) of Eu^{2+} are just embedded in the absorption band (350–650 nm) of Ca_2BN_2F:Eu^{2+}. Thus only energy absorbed in short-wavelength range can be partially transferred to the luminescent centers and then emit blue light. Furthermore, Ca_2BN_2F:Eu^{2+} possesses a small Stokes shift of approximately 2800 cm^{-1} in comparison with calcium–silicon–nitride/oxynitride phosphors (Table 2).

Fig. 7 shows the relationship between the Eu^{2+} concentration and the photoluminescence behaviors of Ca_2BN_2F:Eu^{2+}. Both the excitation and emission profiles have not changed markedly with increasing the Eu^{2+} concentration from x=0.01 to 0.03. The luminescence intensity of Eu^{2+} is significantly decreased by ~65% caused by a higher degree of concentration quenching of Eu^{2+} due to a high ratio of Ca/B=2 from the composition viewpoint. Normally, the emission band of Eu^{2+} can be shifted more or less depending on the composition/structure by increasing the Eu^{2+} concentration [7,11,14,38,39]. Nevertheless, the emission band is almost fixed at about 422 nm in Ca_2BN_2F:Eu^{2+}, say almost independent of the Eu^{2+} concentration. This unusual phenomenon supports the argument that the solubility of Eu^{2+} on the Ca2 site is very low. Additionally, probably the overall possibility of energy transfer between Eu^{2+} to the host is much higher than that in between Eu^{2+} ions themselves in Ca_2BN_2F:Eu^{2+}.

4. Conclusions

Undoped and Eu^{2+}-doped Ca_2BN_2F were synthesized by high temperature solid-state reaction under a N_2–H_2 (10%) atmosphere. X-ray powder diffraction analysis indicated that the obtained $Ca_{2-x}Eu_xBN_2F$ powders are nearly single phase solid solutions. First-principles calculations showed that the valence bands mainly consist of F-2*p*, N-2*p*, and B-2*s*2*p* orbitals (top of the valence band) and the conduction bands are composited of Ca-3*d* states with the calculated energy band gap being about 3.1 eV, in fair agreement with the experimental value of ~3.6 eV. Ca_2BN_2F is confirmed to be an ionic compound because the calculated electronic configurations of Ca-4*s* and Ca-3*d* are almost empty in the valence bands. Ca_2BN_2F:Eu^{2+} has strong absorption in the visible spectral range; however, an absorption center by Eu^{2+} itself (Eu_{Ca}^1N5F1) at about 450 nm does not show luminescence. Ca_2BN_2F:Eu^{2+} emits bright deep blue light under excitation at 339 nm, exhibiting a broad emission band at about 422 nm due to the transition of $4f^6 5d \rightarrow 4f^7$ of Eu^{2+}. This short-wavelength emission of Eu^{2+} is probably mainly attributed to more ionic Eu_{Ca}^2N3F3 center.

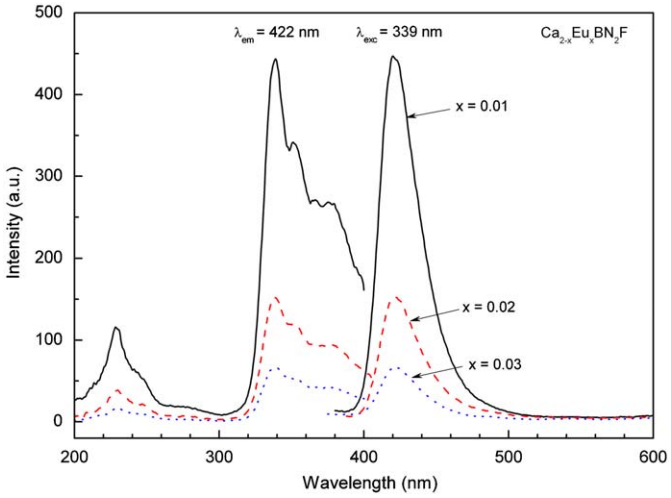

Fig. 7. Excitation and emission spectra of Ca_2BN_2F:Eu^{2+} at different Eu^{2+} concentrations.

References

[1] N.E. Brese, M. O'Keeffe, Crystal chemistry of inorganic nitrides, in: Structure & Bonding, vol. 79, Springer, Berlin, Heidelberg, 1992, pp. 307–378.
[2] R. Marchand, F. Tessier, A. Le Sauze, N. Diot, Int. J. Inorg. Mater. 3 (2001) 1143.
[3] B.V. Beznosikov, J. Struct. Chem. 44 (2003) 885.
[4] R. Niewa, F.J. DiSalvo, Chem. Mater. 10 (1998) 2733.
[5] W. Schnick, H. Huppertz, Chem. Eur. J. 3 (1997) 679.
[6] D.H. Gregory, J. Chem. Soc. Dalton Trans. (1999) 259.
[7] H.T. Hintzen, J.W.H. van Krevel, G. Botty, European Application Patent, EP1104 799 A1, 1999.
[8] H.A. Höppe, H. Lutz, P. Morys, W. Schnick, A. Seilmeier, J. Phys. Chem. Solids 61 (2000) 2001.
[9] R. Mueller-Mach, G. Mueller, M.R. Krames, H.A. Höppe, F. Stadler, W. Schnick, T. Jüestel, P. Schmidt, Phys. Status Solidi (A) 202 (2005) 1727.
[10] [a] R.-J. Xie, N. Hirosaki, Sci. Techno. Adv. Mater. 8 (2007) 588;
[b] R.-J. Xie, N. Hirosaki, M. Mitomo, Oxynitride phosphors, in: W.M. Yen, S. Shionoya, H. Yamamoto (Eds.), Phosphor Handbook, second ed., CRC Press, Taylor & Francis Group, Boca Raton, London, New York, 2006.
[11] Y.Q. Li, J.E.J. van Steen, J.W.H. van Krevel, G. Botty, A.C.A. Delsing, F.J. DiSalvo, G. de With, H.T. Hintzen, J. Alloy Compd. 417 (2006) 273.
[12] Y.Q. Li, G. de With, H.T. Hintzen, J. Solid State Chem. 181 (2008) 515.

[13] Y.Q. Li, N. Hirosaki, R.J. Xie, T. Takeda, M. Mitomo, Chem. Mater. 20 (2008) 6704.
[14] K. Uheda, N. Hirosaki, Y. Yamamoto, A. Naito, T. Nakajima, H. Yamamoto, Electrochem. Solid-State Lett. 9 (2006) 4.
[15] K. Uheda, N. Hirosaki, Y. Yamamoto, H. Yamamoto, Phys. Status Solidi (A) 203 (2006) 2712.
[16] H. Watanabe, H. Yamane, N. Kijima, J. Solid State. Chem. 182 (2008) 1848.
[17] Y.Q. Li, A.C.A. Delsing, G. de With, H.T. Hintzen, Chem. Mater. 17 (2005) 3242.
[18] [a] R.J. Xie, M. Mitomo, K. Uheda, F.F. Xu, Y. Akimune, J. Am. Ceram. Soc. 85 (2002) 1229;
[b] J.W.H. van Krevel, J.W.T. van Rutten, H. Mandal, H.T. Hintzen, R. Metselaar, J. Solid State Chem. 165 (2002) 19.
[19] J.W.H. van Krevel, H.T. Hintzen, R. Metselaar, A. Meijerink, J. Alloys Compd. 268 (1998) 272.
[20] F.E. Rohrer, R. Nesper, J. Solid State Chem. 135 (1998) 194.
[21] Linus Pauling, Nature of the Chemical Bond, third ed., Cornell University Press, Ithaca, New York, 1960.
[22] A.G. Zoltán, M.M. Phillip, J.O. Heston, J.C. Simon, Inorg. Chem. 43 (2004) 3998.
[23] H.A. Höppe, F. Stadler, O. Oeckler, W. Schnick, Angew. Chem. Int. Ed. 43 (2004) 5540.
[24] [a] T. Tsuboi, P. Silfsten, J. Phys. Condens. Mater. 3 (1991) 9163;
[b] W.M. Yen, M.J. Waber, Inorganic Phosphors—Composition, Preparation and Optical Properties, CRC Press, Boca Raton, London, New York, Washington, DC, 2004;
[c] U. Fritzler, G. Schaackz, J. Phys. C Solid State Phys. 9 (1976) L23;
[d] M. Itoh, T. Sakurai, T. Yamakami, J. Fu, J. Lumin. 112 (2005) 161.
[25] U.D. Dzhuzeev, P.E. Ramazanov, Russ. Phys. J. 12 (1969) 890.
[26] H. Chen, H.Z. Zhang, Y. Chen, Y. Liu, C.P. Li, J.S. Williams, J. Aust. Ceram. Soc. 44 (2008) 68.
[27] [a] A.C. Larson, R.B. Von Dreele, Report LAUR 86-748, Los Alamos, National Laboratory, Los Alamos, NM, 2000;
[b] B.H. Toby, J. Appl. Cryst. 34 (2001) 210.
[28] G. Kresse, J. Hafner, Phys. Rev. B 47 (1993) 58.
[29] G. Kresse, J. Furthmuller, Phys. Rev. B 54 (1996) 11169.
[30] J.P. Perdew, S. Burke, M. Ernenrhof, Phys. Rev. Lett. 77 (1996) 3865.
[31] P.E. Blöchl, Phys. Rev. B 50 (1994) 17953.
[32] [a] G. Kresse, D. Joubert, Phys. Rev. B 59 (1999) 1758;
[b] G. Kresse, J. Hafner, Phys. Rev. B 47 (1993) 558;
[c] G. Kresse, J. Hafner, Phys. Rev. B 49 (1994) 14251;
[d] G. Kresse, J. Furthmuller, Comput. Mater. Sci. 6 (1996) 15;
[e] G. Kresse, J. Furthmuller, Phys. Rev. B 54 (1996) 11169.
[33] H.J. Monkhorst, J.D. Pack, Phys. Rev. B 13 (1976) 5188.
[34] C.M. Fang, K.V. Ramanujachary, H.T. Hintzen, G. de With, J. Alloy Compd. 351 (2003) 72.
[35] C.M. Fang, R.A. de Groot, R.J. Bruls, H.T. Hintzen, G. de With, J. Phys. Condens. Matter 11 (1999) 4833.
[36] R.D. Shannon, Acta Crystallogr. A 32 (1976) 751.
[37] T. Balic Zunic, I. Vickovic, J. Appl. Cryst. 29 (1996) 305.
[38] Y.Q. Li, N. Hirosaki, R.J. Xie, T. Takada, K. Shioi, Y. Yamamoto, M. Mitomo, J. Appl. Ceram. Technol., 2009, doi:10.1111/j.1744-7402.2009.02393.x.
[39] G. Blasse, B.C. Grabmaier, Luminescent Materials, Springer, Berlin, 1994.